

Received: 28. October 2022 / Accepted: 02 December 2022 / Published online: 06 December 2022

*plastic, spur gear lattice,
gyroid, additive manufacturing*

Loc Huu NGUYEN^{1,2*}
Khoi Thanh NGUYEN^{1,2}

LIGHTWEIGHT PLASTIC GEAR BODY USING GYROID STRUCTURE FOR ADDITIVE MANUFACTURING

Nowadays, plastic gears are more commonly used. The Triply Periodic Minimal Surfaces (TPMS) structure can perfect the design to reduce weight but still achieve the desired workability criteria. It can also be adjusted more easily and scientifically than the empirical structure optimization based on experience. Currently, the fabrication of gears with complex internal structures such as TPMS is possible thanks to 3D printing technology. This study investigates the mechanical properties of a TPMS structure when applied to Polyetheretherketone (PEEK) plastic gears. The research content includes displacement, deformation, and Von-mises stress to evaluate the stiffness and strength of gears. The structure used to optimize the gear mass is the Gyroid structure, developed in the cylindrical cell map and studied in the paper. The goal of the research is to apply the Gyroid structure to optimize mass while still ensuring gear performance. This study not only offers new insight into the importance of the control variables for TPMS structures but also provides a mass lean process for gear designers. It uses experimental design methods to choose a suitable topology structure, and the final research result is a regression equation, which clearly shows the close relationship between the volume reduction and displacement with the specified control variables of the unit cell. From there, it is possible to determine the proper amount of material reduction while ensuring the working ability of the gear transmission.

1. INTRODUCTION

At present, gears made of non-metallic materials are gradually replacing metal gears in many fields. In 2015, the American Gear Manufacturers Association (AGMA) released a document [1] (reaffirmed June 2020) to review the materials of non-metallic gears. Plastic gears are widely used in new fields as well as gradually replacing steel in applications ranging from automotive components to office automation equipment (printers, scanners, fax machines, ...) [2]. The advantages of plastic gears over metal gears are that the former is competitive in material cost, easier to fabricate, and lighter in density, while its tolerances are not too strict, plus it can withstand a wide range of chemicals, suppress noise due to damping properties, and be self-lubricating due to viscoelastic properties [2]. Therefore, the potential

¹ Faculty of Mechanical Engineering, Ho Chi Minh City University of Technology (HCMUT), Vietnam

² Vietnam National University of Ho Chi Minh City (VNUHCM), Ho Chi Minh City, Vietnam

* E-mail: nhloc@hcmut.edu.vn

<https://doi.org/10.36897/jme/157077>

of non-metallic gears is huge. Except for the case of extremely large power transmissions, the remaining applications of metal gears are gradually being replaced by non-metallic gears. In 2013, the German plastic gear design standard VDI2736 [3] proposed materials with studied mechanical properties suitable for manufacturing gears, failure type, and cause. These standards are quite suitable for general gear design cases; however, according to [4], to select the most suitable gear material, it is necessary to first define all the material data because test data are often inconsistent with actual production conditions.

According to [3], plastic gears have the main types of failure such as melting, crown cracking, root cracking, tooth fatigue, tooth deformation, tooth creep, and abrasion. These failures only occur on the tooth part of the gear, and the material from the transmission shaft to the tooth root is very much left over (Fig. 1), so it is necessary to have a method to reduce excess material and help reduce the weight of the gear. Traditional material reduction methods such as hole punching, body thinning, etc. are mainly based on experience. More scientific methods are needed to achieve maximum volume reduction.

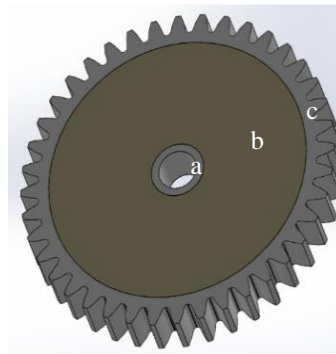


Fig. 1. Gear component: fixed hub (a), gear body (b), tooth ring (c)

The CAD/CAE engineering software has integrated topology optimization algorithms to minimize excess material. However, this software uses traditional topology methods such as Evolutionary Structural Optimization (ESO), Homogenization, Level Set, and Solid Isotropic Material with Penalization (SIMP), which account for a huge amount of computation that leads to a long computation time, difficulty in editing, and still having to use the experience to reshape the details. The topological optimization methods of commercial software only minimize the compliance of the design while constraining the overall volume fraction to a target value [5]. According to [6], the newly created optimal structures will have overhang structures and need to print more support. That support is difficult to remove, and harms the surface detail, costs of material, time, and cost in machining and removal. In addition, this optimal result needs to be converted to a smoothed CAD model before fabrication. Meanwhile, the lattice structure is highly appreciated when optimizing the structure due to its ability to reduce the volume of the structure more easily because it can be controlled by functions and variables.

According to [7], Lattice structures, also known as cellular structures, are those available in nature such as wood, honeycomb, trabecular bone, foam, or butterfly wings [8] that help optimize energy loss. Nature has designed these structures to reach optimal energetic

solutions on a long-term basis that are extremely morphological, lightweight, and optimal in structure and function [9]. To avoid complicating the problem, the lattice structure is represented as unit cells with a defined geometry that repeats periodically in space [10]. There are many ways to classify structures, but the most common is strut-based or triply periodic minimal surfaces (TPMS) [11]. [12] further subdivides TPMS into sheet TPMS and cellular TPMS. There are many different structures and applications of lattice types. However, considering the advantages of mechanical properties to be able to apply them to the gear body, according to [13], TPMS has a higher elastic modulus than strut-based, proving that the TPMS structure has good force dispersion and high strength; there are no areas of stress concentration so the fatigue strength is higher; TPMS structure is better for angular loads. TPMS is less limited in removing excess printing powder inside the structure than strut-based [14]. The characteristics of the TPMS lattice structure have immense potential to optimize the gear structure.

According to [15], [16], TPMS is a surface that is created mathematically, such that they do not have a self-cutting or folding surface. “Triply periodic” means a periodic 3-dimensional structure and “minimal surfaces” mean it minimizes the local surface area within a given boundary limit, such that the average surface curvature at each point is zero. According to [12], there are two different ways to generate a TPMS surface from a mathematical equation; one is to thicken the surface of the TPMS to create a solid structure, called a “sheet” of the TPMS; the other is to fill the volume separated by the TPMS surface, which is called the “cellular” or “skeleton” TPMS. According to [11], Lattice structure design has two steps: unit cell design and pattern design. There are three ways to design a unit cell: primitive-based method, implicit surface-based method, and topology optimization; there are three methods of pattern design: direct patterning, conformal patterning, and topological optimization [16]; a lattice structure can be designed using traditional CAD software, but there will be many limitations related to large degree unit cell repetition to achieve the desired structure, it is possible to use MATLAB [17] or software especially; Currently, the software that supports 3D printing also has unit cell samples in the library.

The choice of lattice topology has a great influence on the geometric accuracy level; Schwarz IWP and Schwarz Diamond configurations have far worse accuracy than Gyroid and Neovius; machinability and mechanical properties are also related because the machinability is too low to affect the actual mechanical properties [18]. Meanwhile, the Gyroid structure can be self-supporting so it is possible to create large-sized unit cells without support [14]. After testing the mechanical properties by simulation and experiment, [19] confirmed that the Gyroid structure has comparable properties with other TPMS structures and is a potential structure in various technological applications. [20] also experimentally confirmed that 3D-printed Gyroid structures are very fast and resistant to loads. [21] applied Lattice structures such as Spiral, Honeycomb, and Gyroid into the mechanical field, intending to reduce the Ti6Al4V gear mass in the position from the transmission shaft to the tooth root, resulting in a Gyroid structure that can withstand 21% more load than solid gear standard gear (DIN 867) despite a 33% reduction in volume. However, [21] uses a Gyroid structure designed with a pattern expanded in a rectangular cell map, so the force distribution is uneven over the entire gear because the structure is subjected to angular force; in the study of [13], the axial and angular forces are different. This study will develop the Gyroid structure according to

the cylindrical coordinate system, distribute the force evenly over the entire gear (Fig. 2), then simulate and evaluate the mechanical properties of the gear. According to [18], choosing the right material is also an important step in the optimal design of a structure; Low-stiffness materials such as β -titanium alloys and PEEK will allow the reduction of the limits of manufacturability and expand design areas where lower stiffness can be achieved. [21] has already used Ti6Al4V, so this study will fill the remaining gap with PEEK plastic material.

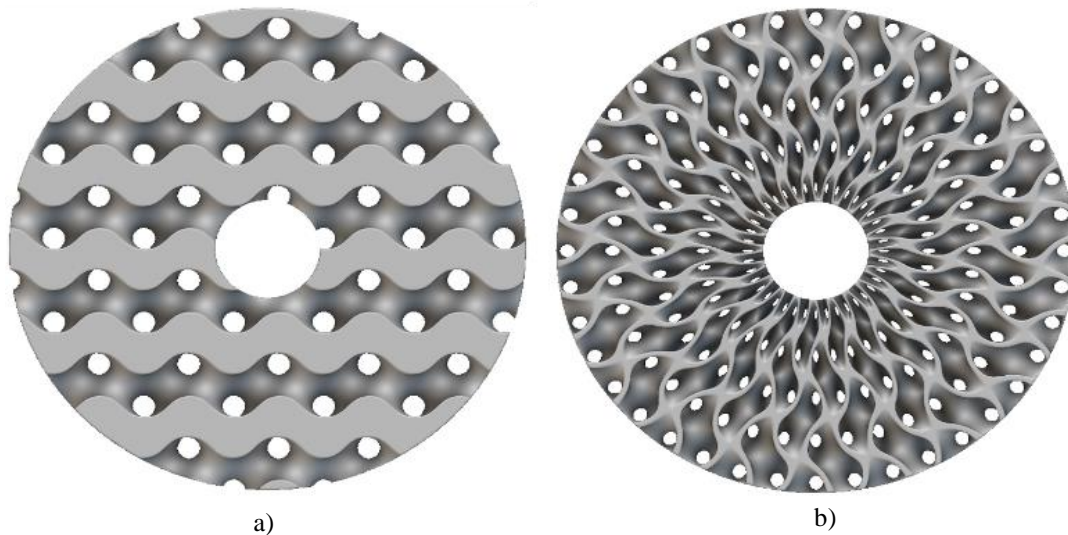


Fig. 2. Gyroid pattern in rectangular cell map (a), cylindrical cell map (b)

2. METHODOLOGY

2.1. LATTICE STRUCTURE

A TPMS structure in a cylindrical cell map can be controlled with these control variables: cell radius, cell height, arc count, and approximate thickness. The first three parameters are used to control the cylindrical cell map (Fig. 3) and the approximate thickness is used to control the unit cell thickness (Fig. 4). The unit cell radius is the size of the unit cell in the u-axis, the unit cell height is the unit cell size in the w-axis, the number of arcs is to divide the v-circle into equal parts and the unit cell is one of them. Approximate thickness is the thickness factor when thickening the TPMS plane. Only the number of arcs must be selected as a positive integer, and the remaining input parameters will be optional according to the machining capabilities of the 3D printing device. Volume reduction is expressed in:

$$R_v = 1 - V/V_0 \quad (1)$$

where V is the volume of the TPMS part, V_0 is the volume of the full part

There are 6 TPMS structures used in this study, including SplitP; Neovius; Diamond; Schwarz; Lininoid; and Gyroid to evaluate the influence of the structure on the mechanical properties of the gear as shown in Fig. 5.

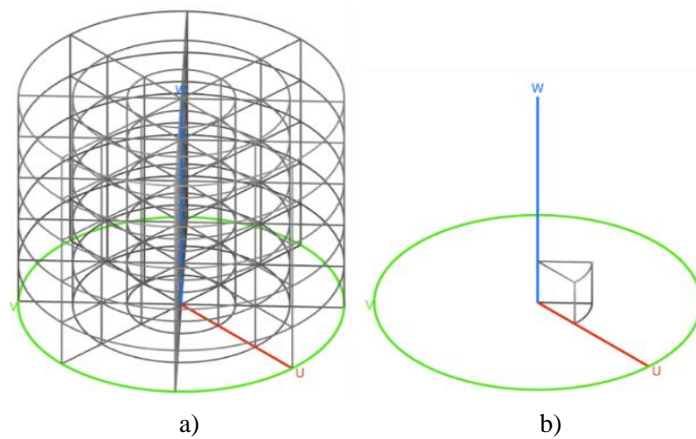


Fig. 3. Cylindrical cell map with cell radius: 2 mm; cell height: 2 mm and arc count: 8 (a), One unit cell in the cylindrical cell map (b)

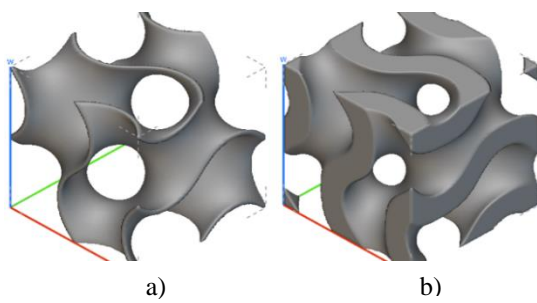


Fig. 4. Gyroid unit cell with thickness: 0.5 mm (a), 2.5 mm (b)

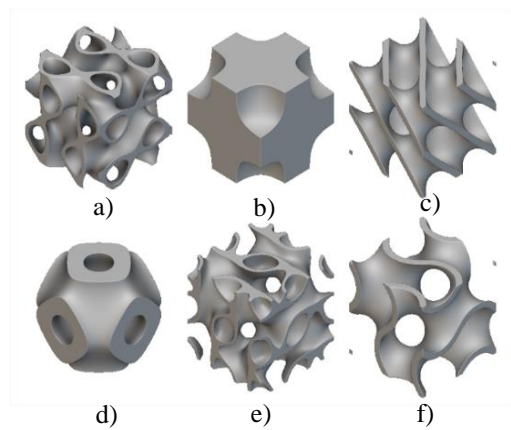


Fig. 5. SplitP (a); Neovius (b); Diamond (c); Schwarz (d); Lininoid (e); Gyroid (f)

2.2. FINITE ELEMENT MODEL

The gear is used to apply TPMS structure to the gear body area (Fig. 6) and apply FE Robust Tetrahedral Mesh to both solid gear and TPMS gear (Fig. 7). The simulation is simple by constraining a part of any tooth and applying torque to the fixed hub (Fig. 8). The simulation results are shown in Fig. 9.

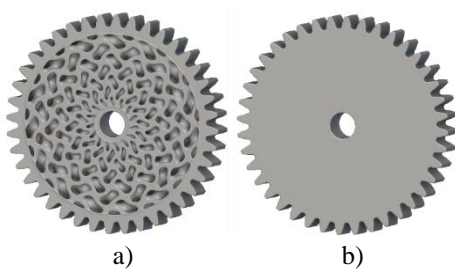


Fig. 6. TPMS gear (a), Solid Gear (VDI 2736) (b)

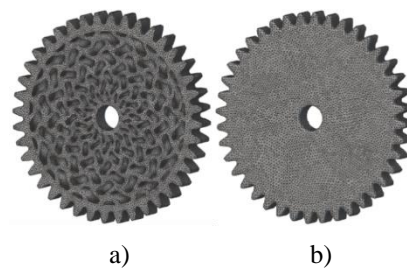


Fig. 7. FE Robust Tetrahedral Mesh FE TPMS Gear (a), FE Solid Gear (b)

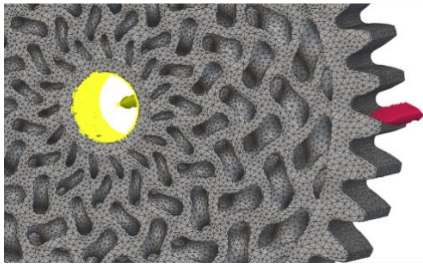


Fig. 8. Tooth constraint (red) and torque (yellow)

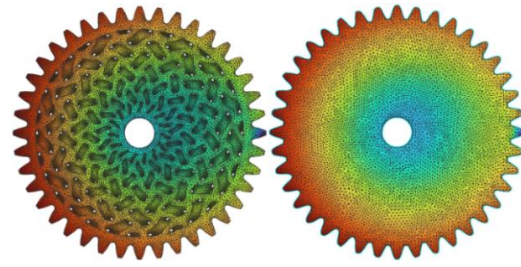


Fig. 9. Simulation result

2.3. INTRODUCTION OF DESIGN OF EXPERIMENTAL METHODS

Taguchi method allows for studying the influence of factors on a response with the minimum number of experiments that are needed, from which the proper structure can be selected. This method is particularly suitable when there are too many factors, each of which has many different levels of values, and the factors might be just names, not numbers. Therefore, the Taguchi method is used for preliminary experiments when there are 5 factors affecting gears; the TPMS structure factor must take 6 levels of values to evaluate, and the others take 3 value levels.

Face Centered Central Composite Design (FCCCD) method can describe the properties of the research object in the entire design space relatively well. In Central Composite Design (FCCCD, Box-Wilson, Box-Hunter), FCCCD helps researchers conduct fewer experiments and levels of values but still get the regression equation with ensured accuracy and compatibility [22]. With this method, it is easy to obtain the quadratic regression equation and show the correlation between the factors for each response. However, the factors must have the same number of levels of values, and all must be real. Therefore, the FCCCD method is used immediately after the Taguchi method when a suitable structure has been found.

3. RESEARCH RESULT

3.1. GEAR DESIGN

The simulation material for the gear is PEEK (VDI2736) with Young's Modulus: 3580 N/mm^2 , Poisson's ratio: 0.4, and Density: 1300 kg/m^3 . The gear size for the Taguchi method: normal module $m = 2 \text{ mm}$, normal pressure angle $\alpha = 20^\circ$, number of teeth $n = 20$, face width $b = 10 \text{ mm}$, torque = 5 Nm. The gear size for the FCCCD method: normal module $m = 1 \text{ mm}$, normal pressure angle $\alpha = 20^\circ$, number of teeth $n = 40$, face width $b = 5 \text{ mm}$, torque $T = 1 \text{ Nm}$.

3.2. STRUCTURE SELECTION ACCORDING TO TAGUCHI ANALYSIS

TPMS structure types and control variables that affect volume reduction should be selected as factors to evaluate their influence on the mechanical properties of gears. TPMS includes 6 structures, and the value range of control variables is selected to ensure that

the volume reduction is not zero, and the arc count must be chosen as an integer. This study will evaluate the influence of factors on volume reduction (RV), displacement (D), deformation (ε), and stress (σ) of gears applying TPMS structure compared with solid gears through the Taguchi method. It uses Taguchi Design L18, where smaller is better, for 5 factors ($6^1; 3^4$) as shown in Table 1, then runs simulations and obtains results as in Table 2.

Table 1. Factors and level values in the Taguchi method

Factor	Level Values
Type	Gyroid (Gy); Schwarz (Sh); Diamond (Di); Lininoid (Li); SplitP (Sp); Neovius (Ne)
Radius (R) (mm)	6; 7; 8
Height (H) (mm)	6; 7; 8
Arc (A)	10; 15; 20
Thickness (T) (mm)	1.1; 1.3; 1.5

Table 2. Taguchi method table and simulation result

Type	Radius (mm)	Height (mm)	Arc	Thickness (mm)	Volume reduction	Displacement (mm)	Strain (%)	Stress (MPa)
Full					0	0.049749	0.0103929	75.73610
Gy	6	6	10	1.1	0.2507	0.076539	0.0112524	73.01830
Gy	7	7	15	1.3	0.2188	0.069565	0.0088766	63.41840
Gy	8	8	20	1.5	0.1935	0.067387	0.0084463	54.14320
Sh	6	6	15	1.3	0.0898	0.054998	0.0084348	54.03750
Sh	7	7	20	1.5	0.0750	0.054669	0.0088226	57.00000
Sh	8	8	10	1.1	0.1987	0.066700	0.0101607	67.29610
Di	6	7	10	1.5	0.1756	0.063320	0.0122584	62.71220
Di	7	8	15	1.1	0.2239	0.071016	0.0090778	69.19430
Di	8	6	20	1.3	0.1678	0.062742	0.0094657	55.60290
Li	6	8	20	1.3	0.1303	0.061257	0.0102563	65.83920
Li	7	6	10	1.5	0.1368	0.059382	0.0097182	57.95600
Li	8	7	15	1.1	0.1762	0.064382	0.0103132	54.38242
Sp	6	7	20	1.1	0.1676	0.063360	0.0077902	57.71870
Sp	7	8	10	1.3	0.2034	0.066772	0.0095716	53.89130
Sp	8	6	15	1.5	0.1291	0.058267	0.0080866	52.69380
Ne	6	8	15	1.5	0.0461	0.052363	0.0085396	52.61090
Ne	7	6	20	1.1	0.0602	0.053128	0.0092962	51.34910
Ne	8	7	10	1.3	0.0903	0.056121	0.0103986	68.45030

Table 3. Taguchi Analysis: Volume reduction versus Type, Radius, Height, Arc, Thickness

Level	Type	R	H	A	T
1	2.17	1.37	1.32	1.70	1.74
2	1.14	1.47	1.43	1.41	1.43
3	1.83	1.52	1.60	1.25	1.19
4	1.39				
5	1.59				
6	0.59				
Delta	1.58	0.15	0.28	0.45	0.56
Rank	1	5	4	3	2

Table 4. Taguchi Analysis: Displacement versus Type, Radius, Height, Arc, Thickness

Level	Type	R	H	A	T
1	22.97	24.22	24.38	23.81	23.68
2	24.65	24.15	24.20	24.24	24.20
3	23.66	24.09	23.88	24.41	24.58
4	24.20				
5	24.05				
6	25.38				
Delta	2.41	0.13	0.50	0.60	0.90
Rank	1	5	4	3	2

Table 5. Taguchi Analysis: Strain versus Type, Radius, Height, Arc, Thickness

Level	Type	R	H	A	T
1	40.49	40.33	40.61	39.56	40.37
2	40.81	40.70	40.32	41.05	40.47
3	39.85	40.51	40.62	40.94	40.71
4	39.92				
5	41.46				
6	40.56				
Delta	1.62	0.37	0.30	1.49	0.34
Rank	1	3	5	2	4

Table 6. Taguchi Analysis: Stress versus Type, Radius, Height, Arc, Thickness

Level	Type	R	H	A	T
1	-36.0	-35.7	-35.1	-36.1	-35.8
2	-35.4	-35.4	-35.6	-35.2	-35.6
3	-35.9	-35.3	-35.6	-35.1	-35.0
4	-35.5				
5	-34.8				
6	-35.1				
Delta	1.2	0.3	0.5	1.0	0.8
Rank	1	5	4	2	3

Table 7. TPMS structures with the same control variables

Type	Radius (mm)	Height (mm)	Arc	Thickness (mm)	Volume reduction	Displacement (mm)	Strain (%)	Stress (MPa)
Full					0	0.0497	0.0104	75.7361
Gy	6	6	20	1.5	0.1521	0.0617	0.0111	66.4193
Sh	6	6	20	1.5	0.0499	0.0524	0.0087	60.2903
Di	6	6	20	1.5	0.1075	0.0571	0.0082	54.3002
Ne	6	6	20	1.5	0.0227	0.0509	0.0079	60.3908
Sp	6	6	20	1.5	0.0816	0.0552	0.0081	58.3729
Li	6	6	20	1.5	0.0900	0.0567	0.0081	54.8109

From Taguchi analysis (Table 3, Table 4, Table 5, Table 6, and Fig. 10, Fig 11), it can be seen that the type of structure has the most significant influence on displacement, strain,

and stress; then come the thickness and arc count. Although the SplitP structure has advantages in terms of stress and strain, it is not suitable for volume reduction. By conducting simulations with the same control variables, it was found that although the stress, strain, and displacement of the SplitP structure were good compared with the full gear, it did not reduce much volume (Table 7).

The study continues to evaluate Displacement/Volume reduction, Strain/Volume reduction, and Stress/Volume reduction (Fig. 12) to find a suitable configuration. From the Taguchi analysis, it can be concluded that the Gyroid structure satisfies the need for optimum gear mass when achieving lower displacement, strain, and stress to volume reduction ratios than other structures.

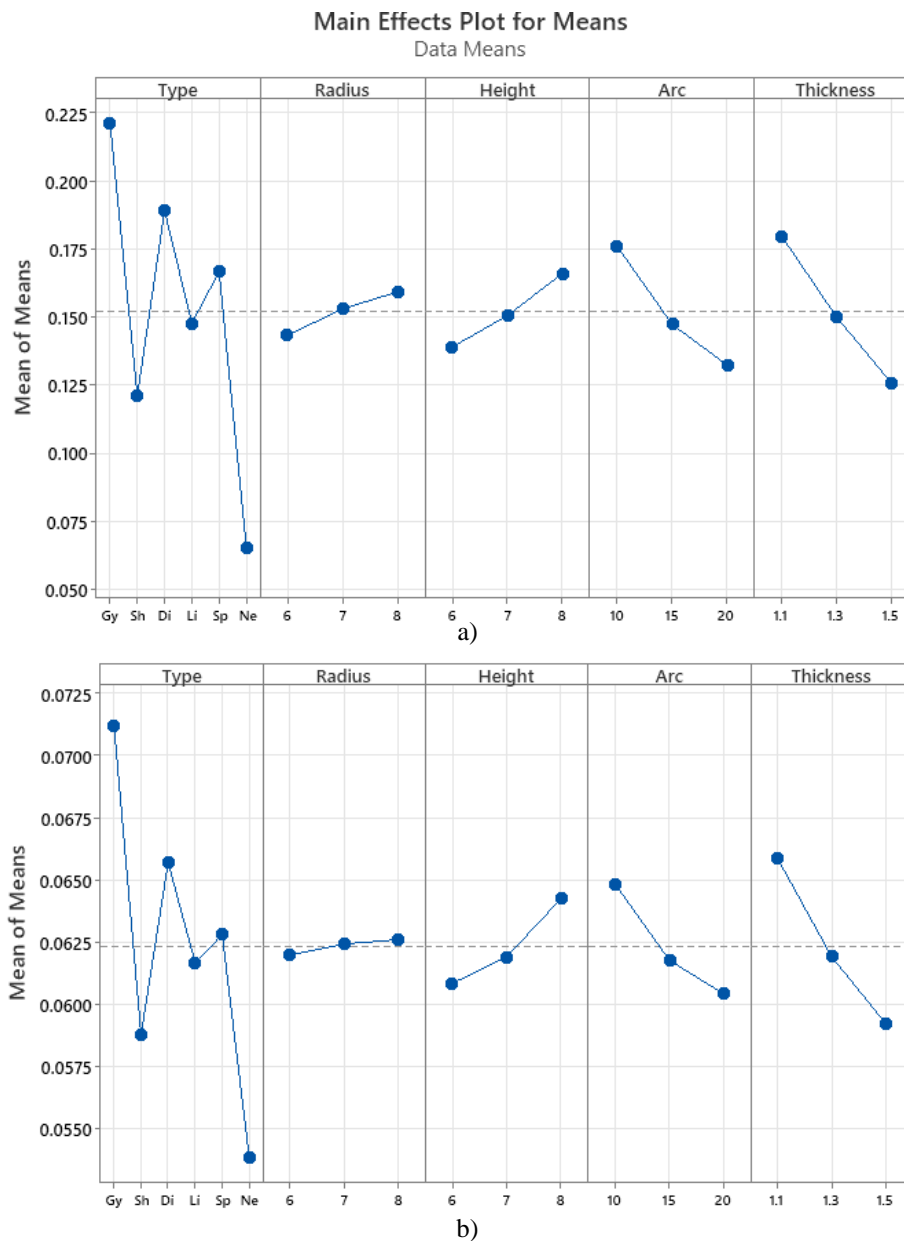


Fig. 10. Diagram for Taguchi analysis: volume reduction (a), displacement (b)

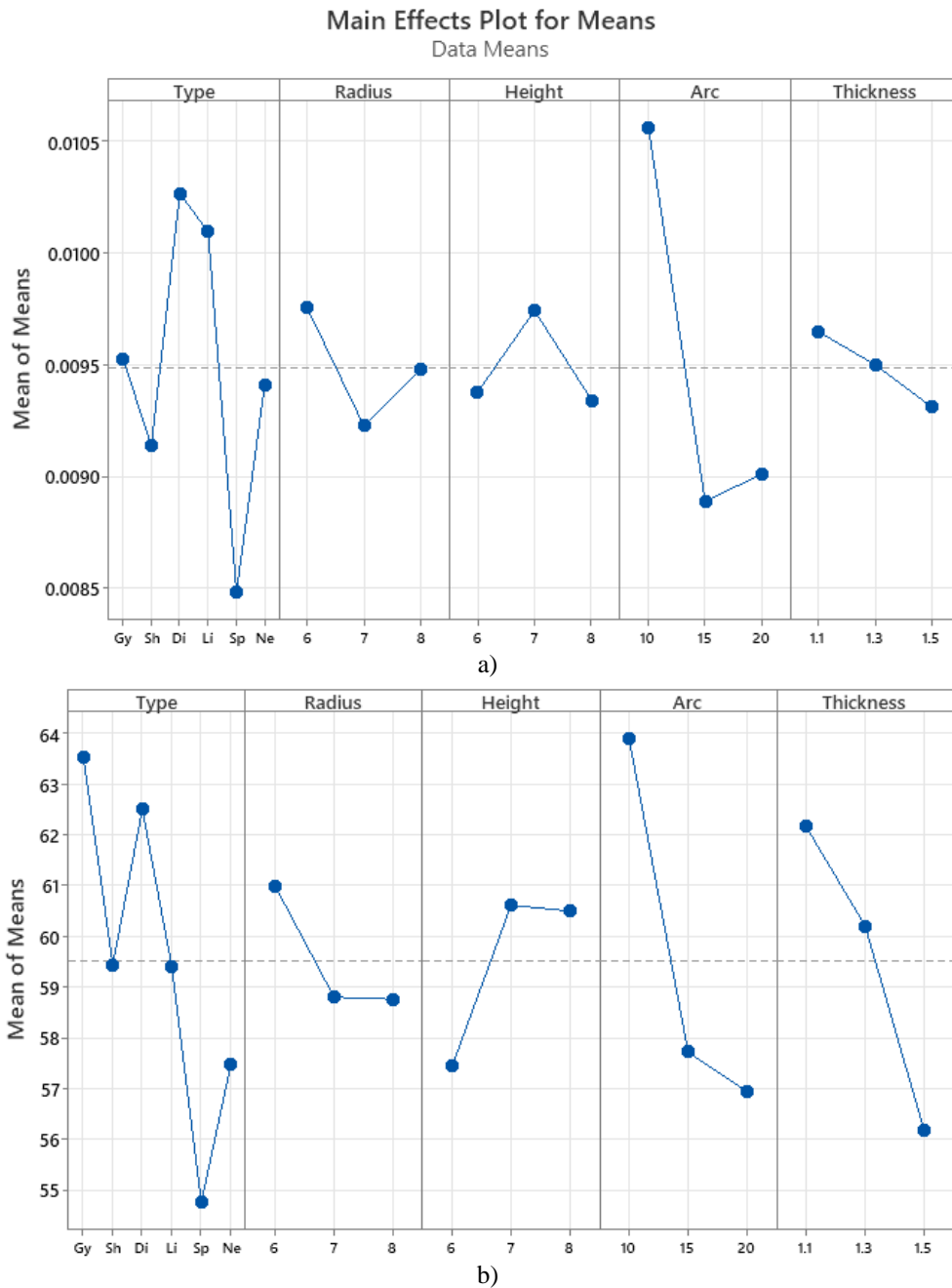
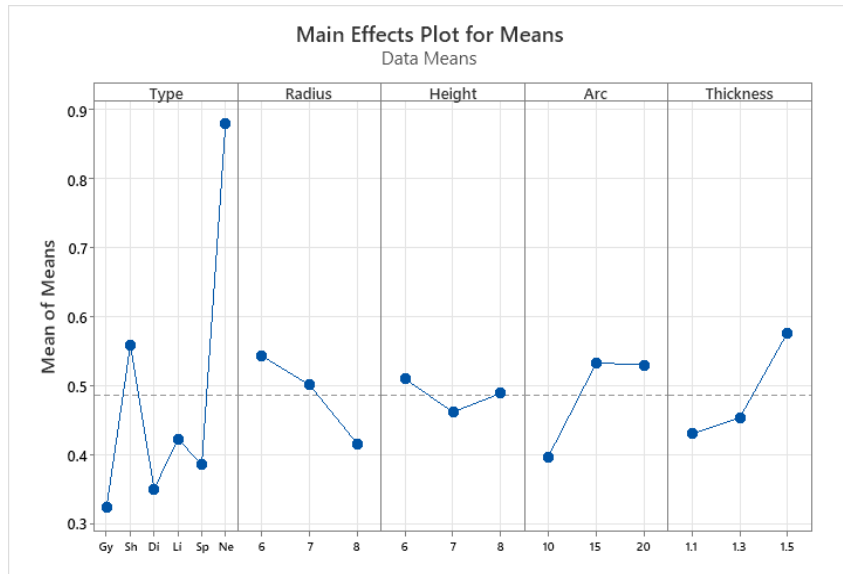


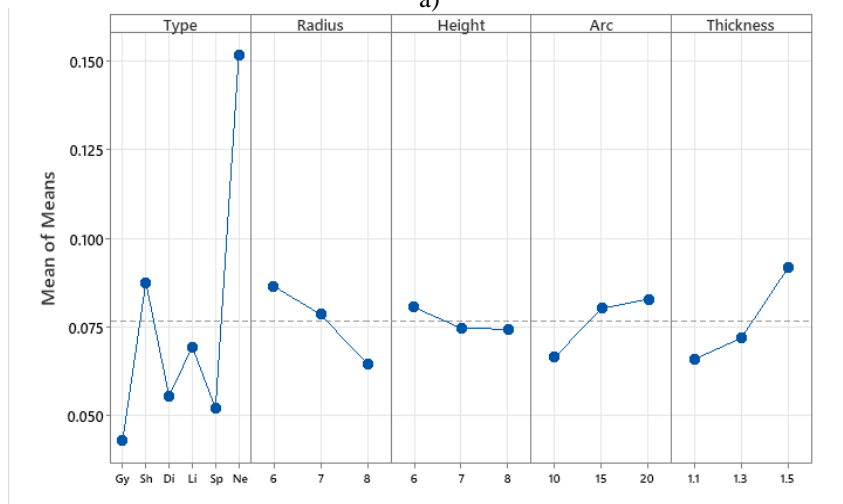
Fig. 11. Diagram for Taguchi analysis: strain (a), stress (b)

3.3. RESPONSE SURFACE ANALYSIS FOR OPTIMIZATION

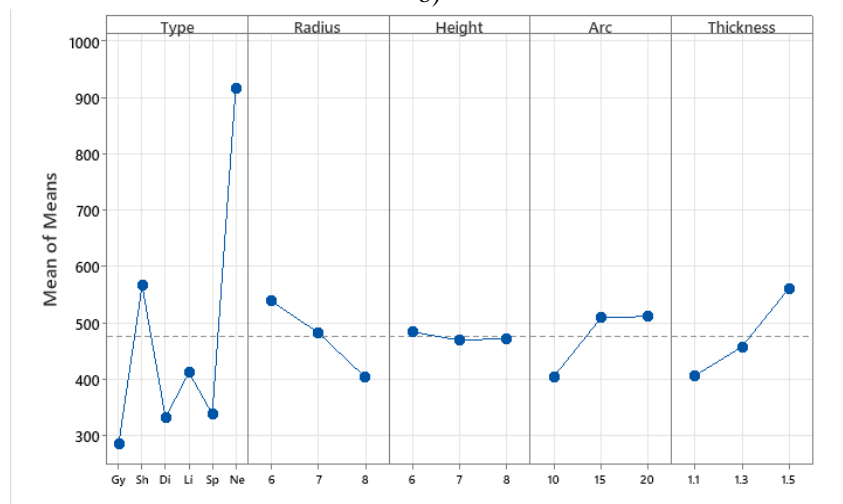
After proving to Taguchi that the Gyroid structure is the most suitable type for reducing the mass in the gear, the remaining 4 factors have not been studied for their influence on the mass of the structure. Therefore, the FCCCD method is implemented for gears applying a Gyroid structure with those 4 remaining factors for further study as shown in Table 8. Because of the finite element simulation, only 1 iteration was performed, and thus 25 experiments in total. The results are shown in Table 9.



a)



b)



c)

Fig. 12: Taguchi analysis: displacement/volume reduction (a), strain/volume reduction (b), stress/volume reduction (c)

Table 8. FCCCD factors and value levels

N	Factor	Name	Value levels			Intervals
			-1	0	+1	
1	<i>R</i>	Radius (mm)	3	4	5	1
2	<i>H</i>	Height (mm)	3	4	5	1
3	<i>A</i>	Arc	10	15	20	5
4	<i>T</i>	Thickness (mm)	1.1	1.3	1.5	0.2

Table 9. FCCCD method table and simulation result

No.	Radius (mm)	Height (mm)	Arc	Thickness (mm)	Volume reduction	Displacement (mm)	D/D_0^*	Strain (%)	Stress (MPa)
	Full Gear				0.0000	0.0277	1.0000	0.00734	51.6650
1	3	3	10	1.1	0.3301	0.0402	1.4507	0.00619	36.9082
2	5	3	10	1.1	0.3945	0.0425	1.5359	0.00712	42.4398
3	3	5	10	1.1	0.3953	0.0513	1.8518	0.00667	34.2970
4	5	5	10	1.1	0.4482	0.0519	1.8740	0.00702	49.3335
5	3	3	20	1.1	0.2189	0.0338	1.2211	0.00671	34.9491
6	5	3	20	1.1	0.3032	0.0382	1.3792	0.00693	51.1541
7	3	5	20	1.1	0.3034	0.0414	1.4954	0.00670	44.8669
8	5	5	20	1.1	0.3721	0.0458	1.6527	0.00710	36.2507
9	3	3	10	1.5	0.1758	0.0319	1.1502	0.00607	37.2256
10	5	3	10	1.5	0.2665	0.0352	1.2710	0.00607	45.6617
11	3	5	10	1.5	0.2669	0.0396	1.4291	0.00679	40.4459
12	5	5	10	1.5	0.3421	0.0417	1.5050	0.00904	74.8633
13	3	3	20	1.5	0.0478	0.0285	1.0290	0.00640	38.8290
14	5	3	20	1.5	0.1416	0.0308	1.1113	0.00579	35.3452
15	3	5	20	1.5	0.1419	0.0322	1.1640	0.00579	33.6705
16	5	5	20	1.5	0.2361	0.0369	1.3322	0.00724	42.9839
17	3	4	15	1.3	0.2328	0.0352	1.2714	0.00592	31.6941
18	5	4	15	1.3	0.3148	0.0394	1.4217	0.00857	57.2505
19	4	3	15	1.3	0.2334	0.0344	1.2422	0.00591	33.5628
20	4	5	15	1.3	0.3161	0.0412	1.4863	0.00747	53.4773
21	4	4	10	1.3	0.3412	0.0413	1.4921	0.00762	50.4214
22	4	4	20	1.3	0.2336	0.0356	1.2840	0.00638	39.9536
23	4	4	15	1.1	0.3538	0.0418	1.5085	0.00730	46.7193
24	4	4	15	1.5	0.2085	0.0340	1.2259	0.00561	46.4760
25	4	4	15	1.3	0.2820	0.0374	1.3495	0.00635	36.6595

* D/D_0 is the displacement of the volume-reduced gear divided by the solid gear

Based on the analysis results, it is found that the regression equation between volume reduction (2) and displacement (3) for factors has very high compatibility, *R*-sq is 99.96% and 99.4% (Table 10), respectively. However, the compatibility of stress and strain was not high, at less than 70% (Table 10). But obviously, most gears that do not respond to strain and stress are those with volume reductions higher than 30%, so the largest amount of material can be cut without affecting the mechanical properties counted as less than 30%. When using the cubic regression equation to test the correlation of volume reduction and displacement, the results obtained are that these two values have a correlation level of more than 90% (Fig. 13).

$$\begin{aligned}
 Rv = & 0.6129 + 0.0631R + 0.0564H - 0.01477A - 0.467T \\
 & - 0.00726 R2 - 0.00634 H2 + 0.000253A2 + 0.0024T2 \\
 & - 0.002629RH + 0.000722RA + 0.02613RT \\
 & + 0.000707HA + 0.02596HT - 0.007090AT
 \end{aligned} \tag{2}$$

$$\begin{aligned}
 \text{Displacement} = & 0.0660 + 0.00175R + 0.00810H - 0.002146A - 0.0377T \\
 & - 0.000207R2 + 0.000283H2 + 0.000038A2 + 0.0091T2 \\
 & - 0.000040RH + 0.000091RA + 0.000211RT \\
 & - 0.000121HA - 0.003622HT + 0.000424AT
 \end{aligned} \tag{3}$$

Table 10. R-sq of the regression equation of the responses

No.	Response	S	R-sq	R-sq(adj)	R-sq(pred)
1	Volume reduction	0.0028471	99.96%	99.90%	99.69%
2	Displacement	0.0006918	99.40%	98.56%	95.31%

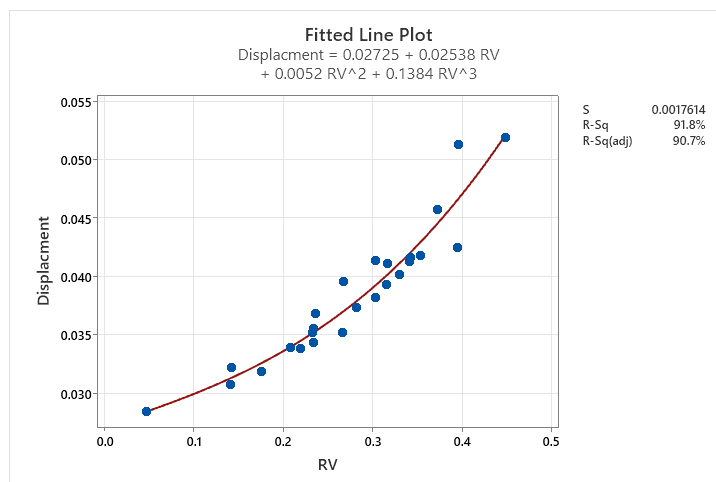


Fig. 13. Regression cubic line plot of volume reduction and displacement

From Fig. 14 it can be seen that thickness has a great influence on both volume reduction and displacement, so thickness should only be adjusted so that the volume reduction is greater than 10%, but it should not be reduced too much because of the affection of the gear stiffness. The radius of the unit cell does not affect the volume reduction and displacement too much, so it can be kept the same or adjusted higher. The arc count has a second effect on volume reduction but only a third effect on displacement, so this parameter is only selected to ensure

the volume reduction is greater than 10%, Choosing it too high will not reduce the volume reduction much but will affect the stiffness. The unit cell height has a third effect on volume reduction but a second effect on displacement, so it should be kept as small as possible, just ensuring the structure is still within manufacturability.

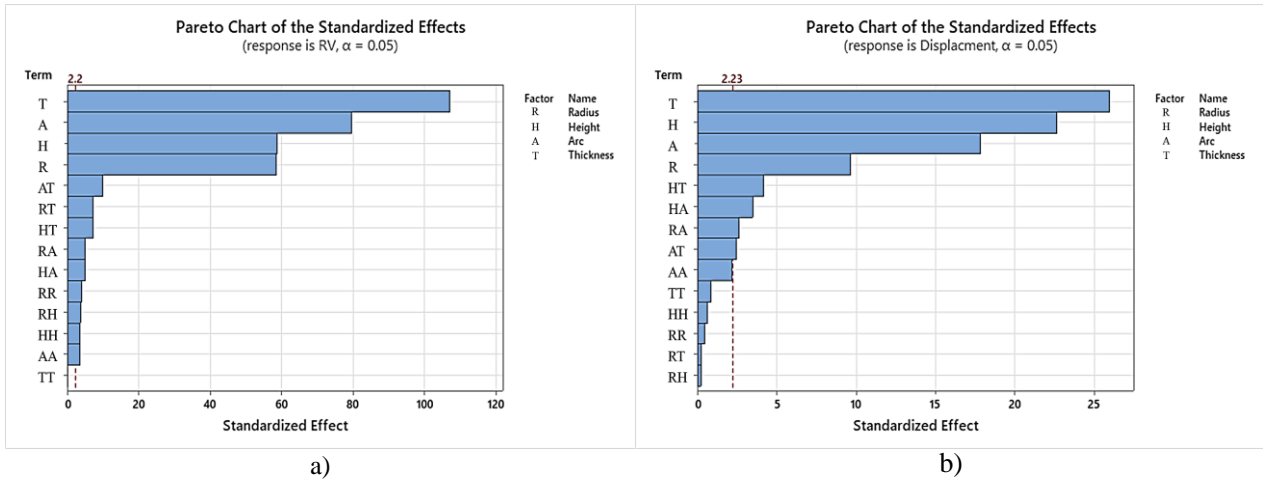


Fig. 14. Pareto Chart evaluates the significance of the factors for the regression equation of volume reduction (a) and displacement (b)

Another FCCCD is conducted with the new control variables. Table 11 contains the factors and the range of values for the second FCCCD implementation, but this time the value ranges of the factors are re-selected according to the result drawn from the previous FCCCD and obtained the results as Table 12.

Table 11. FCCCD factors and value levels (second times)

N	Factor	Name	Value levels			Step
			-1	0	+1	
1	<i>R</i>	Radius (mm)	6	7	8	1
2	<i>H</i>	Height (mm)	0.9	1.4	1.9	0.5
3	<i>A</i>	Arc	25	30	35	5
4	<i>T</i>	Thickness (mm)	0.7	0.8	0.9	0.1

Table 12. FCCCD method table and simulation result (second time)

No.	<i>R</i>	<i>H</i>	<i>A</i>	<i>T</i>	R_V	D	D/D_0^*	ϵ	σ
0	Full Gear				0	0.0277	1	0.00734	51.6650
1	6	0.9	25	0.7	0.3197	0.0355	1.2823	0.00597	37.3510
2	8	0.9	25	0.7	0.3575	0.0371	1.3403	0.00635	34.2808
3	6	1.9	25	0.7	0.4136	0.0443	1.5988	0.00813	41.1018
4	8	1.9	25	0.7	0.4429	0.0458	1.6517	0.00829	66.4848
5	6	0.9	35	0.7	0.2680	0.0340	1.2289	0.00565	35.4177

6	8	0.9	35	0.7	0.3108	0.0358	1.2915	0.00649	44.2880
7	6	1.9	35	0.7	0.3739	0.0433	1.5622	0.00641	44.1213
8	8	1.9	35	0.7	0.4081	0.0448	1.6162	0.00671	37.2650
9	6	0.9	25	0.9	0.1952	0.0306	1.1060	0.01010	43.2814
10	8	0.9	25	0.9	0.2464	0.0321	1.1583	0.00599	34.0016
11	6	1.9	25	0.9	0.3191	0.0384	1.3871	0.00651	41.0374
12	8	1.9	25	0.9	0.3580	0.0401	1.4486	0.00648	39.5233
13	6	0.9	35	0.9	0.1321	0.0298	1.0746	0.00646	42.2791
14	8	0.9	35	0.9	0.1862	0.0307	1.1100	0.00547	35.9770
15	6	1.9	35	0.9	0.2668	0.0365	1.3163	0.00701	53.1921
16	8	1.9	35	0.9	0.3117	0.0393	1.4172	0.00801	57.0699
17	6	1.4	30	0.8	0.2990	0.0373	1.3481	0.00689	45.1102
18	8	1.4	30	0.8	0.3391	0.0381	1.3747	0.00623	38.7438
19	7	0.9	30	0.8	0.2518	0.0328	1.1849	0.00833	45.2538
20	7	1.9	30	0.8	0.3616	0.0422	1.5220	0.00636	36.0364
21	7	1.4	25	0.8	0.3455	0.0385	1.3881	0.00699	47.1097
22	7	1.4	35	0.8	0.2974	0.0374	1.3491	0.00632	44.3849
23	7	1.4	30	0.7	0.3726	0.0404	1.4600	0.01014	51.8304
24	7	1.4	30	0.9	0.2667	0.0352	1.2718	0.00629	45.0575
25	7	1.4	30	0.8	0.3202	0.0376	1.3587	0.00651	56.6285

* D/D_0 is the displacement of the volume-reduced gear divided by the solid gear

The second time, it can be seen that to achieve a displacement of less than 20%, the volume reduction must be less than 26% (Table 12 No. 10 and No. 19); to achieve a displacement of less than 11%, the volume reduction must be less than 20% (Table 12 No. 9, No. 13 and No. 14). Volume reduction below 30% will not exceed the strain and stress of solid gears. The compatibility of factors for volume reduction and displacement regression equation, (4) and (5), has increased (99.99% and 99.64%); however, the compatibility of factors for stress and strain decreased sharply (Table 13). The correlation between volume reduction and displacement stays above 90%. (Fig. 15). Fig. 16 shows that now the height of the unit cell has the most significant influence on both volume reduction and displacement.

$$\begin{aligned}
 R_V = & 0.7081 + 0.01131R + 0.14334H - 0.00691A - 0.703T \\
 & - 0.000951R^2 - 0.05330H^2 + 0.000059A^2 - 0.0349T^2 \\
 & - 0.004845RH + 0.000233RA + 0.02817RT \\
 & + 0.001214HA + 0.14146HT - 0.006133AT
 \end{aligned} \tag{4}$$

$$\begin{aligned}
 \text{Displacement} = & 0.0376 + 0.00176R + 0.01537H - 0.000332A - 0.0194T \\
 & - 0.000135R^2 - 0.00142H^2 + 0.000003A^2 - 0.0009T^2 \\
 & + 0.000212RH + 0.000010RA + 0.00039RT \\
 & + 0.000005HA - 0.00574HT - 0.000026AT
 \end{aligned} \tag{5}$$

Table 13. R-sq of the regression equation of the responses (second time)

No.	Response	S	R-sq	R-sq(adj)	R-sq(pred)
1	Volume reduction	0.0010578	99.99%	99.98%	99.95%
2	Displacement	0.0004142	99.64%	99.13%	97.57%

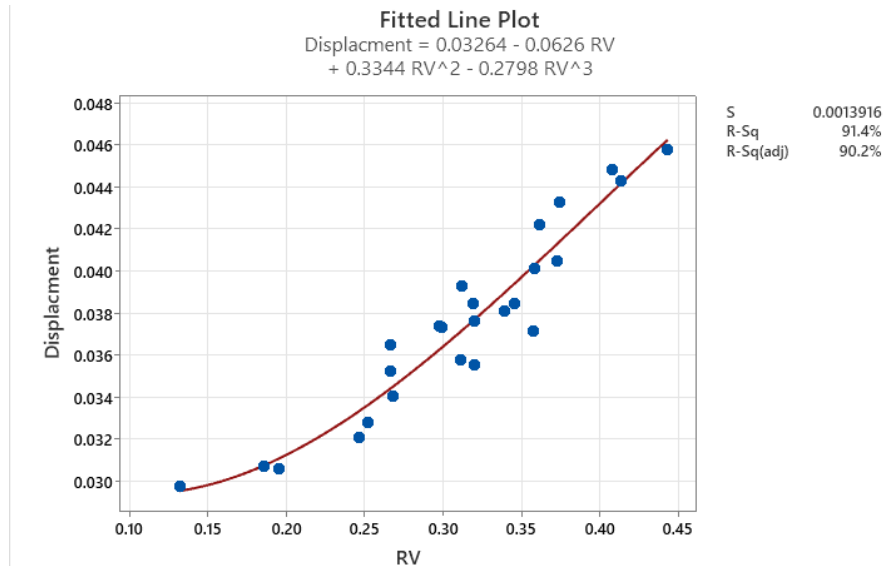


Fig. 15. Regression cubic line plot of volume reduction and displacement (second times)

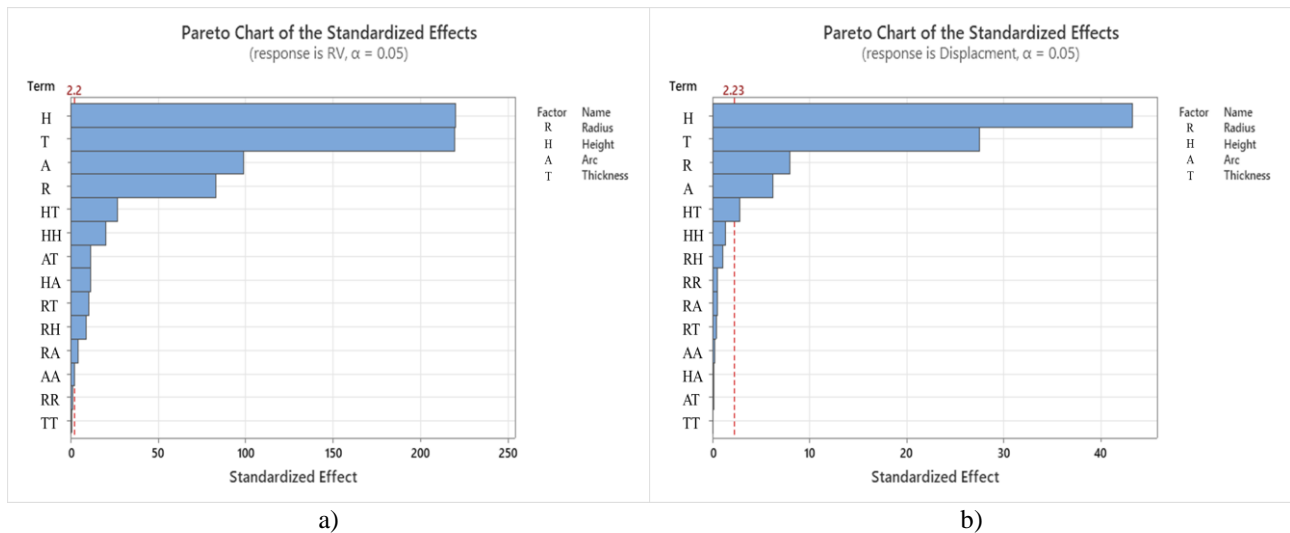


Fig. 16. Pareto Chart evaluates the significance of the factors for the regression equation of volume reduction (a) and displacement (b) (second times)

4. ANALYSIS AND DISCUSSION

Gears when applying the Gyroid structure to reduce mass can reduce stress and strain, showing the potential to increase the strength and stiffness of the gears. At present, it is necessary to find out the correlation rule between the generated stress and strain and

the design variables. In some cases, the gear stress and strain after volume reduction are higher than the solid gear, but if the volume reduction is kept below 30%, the stress and strain will be lower than that of the solid gear.

The displacement in the gear, on the other hand, is closely related to the design variables (R-sq over 99%) and the volume reduction (R-sq above 90%). If compared with another study by [23] for traditional gear reduction methods such as holes or ribbed; then analysing the similarity with Fig. 13 and Fig. 15, it can be concluded that even though the new topology structure is applied to reduce the mass, the volume reduction still influences the gear displacement and stiffness; however, the stiffness can be adjusted by reducing the unit cell height and reducing the volume loss moderately through the remaining input parameters for higher stiffness. This adjustment is more scientific with the regression equation being derived from the FCCCD method, which is controllable, and completely independent of experience. According to the results of [23], it can be seen that the traditional method has about 24% larger displacement than the solid gear, but the material reduction is only about 15%. While (Table 12 No. 10) shows that this new topology reduces the amount of material by over 24% with only 16% larger displacement than the solid gear and also has lower stress and strain.

When observing the first Pareto chart of volume reduction and displacement (Fig. 14), it can be seen that all four factors have an influence, but the degree of influence is different. Thickness has the greatest influence on displacement and volume reduction, the larger the thickness, the lower the displacement and the lower the volume loss. To reduce mass, increasing the thickness to increase the gear stiffness is not the optimal solution, so only a suitable thickness should be selected. It should be thick enough to achieve high stiffness but thin enough to achieve the desired volume reduction. The radius of the unit cell has the least effect; the larger the radius, the less displacement and volume reduction will decrease, but not much. This can be considered as a parameter to fine-tune the amount of mass to be reduced of the gear accordingly. Two notable parameters here are the arc count and the height of the unit cell. The number of arcs is the second most influential factor for the volume reduction but only the third effect for displacement, i.e., increasing the number of arcs too high leads to a significant increase in volume but not much stiffness for the gear. This means that increasing the number of arcs to increase the stiffness of the gear is not beneficial, and only the proper number of arcs should be selected. The height of the unit cell has the third effect on volume reduction but the second most significant effect on displacement, so decreasing the height results in a slight increase in volume but an enormous improvement in displacement. This shows that lowering the height of the unit cell and then adjusting the volume reduction through other variables will help improve the desired gear displacement and ensure the amount of material.

When the second Pareto chart (Fig. 16) is observed, the re-selected variables make the height of the unit cell become the greatest influence on displacement and volume reduction. Because the chosen thickness step is small, the thickness influence decreases. The order of selection of control variables when applying the Gyroid structure to the gear is drawn as follows, first selecting the parameters with the goal of the thickness as small as possible but still ensuring the machinability; then recalculating the volume reduction. If not suitable, the unit cell height and thickness can be adjusted to suit the needs, and the other two parameters can be kept the same. The adjustment of control variables is of great importance

in the ability to shape the TPMS structure. If the control variables are not adjusted properly, they cause many errors such as structural errors (Fig. 17), meshing errors, and algorithm errors. Those errors are not yet controllable, but they rarely happen. Also, the change to eliminate errors is simple by just randomly increasing and decreasing the control variables, especially the radius of the unit cell or the arc count.

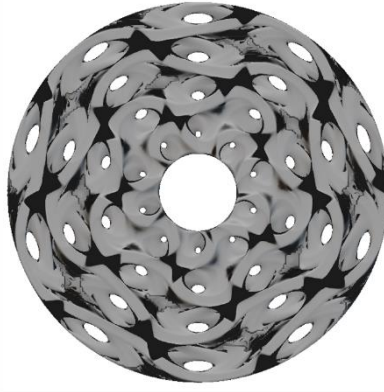


Fig. 17. Error when choosing arc count $A = 5$ (black areas appear)

To account for how changing the height of the unit cell affects the displacement, the Gyroid unit cell must be revised. A cell has 2 position types: 450 and 900 as shown in Fig. 18. When the force is applied in the w direction, position 900 will be subjected to tension and compression at the centre, so the displacement will be lower than position 450. This angle only occurs when the two dimensions w and u of the unit cell are equal (i.e., like a square), as the w dimension increases, the angle of 450 will increase closer to 900 and vice versa. Therefore, for the gear to become stiffer, the optimal area needs to have many positions with an angle of 900 in the bearing direction, and the remaining positions gradually increase to 900. The decrease in the height of the Gyroid unit cell in a cylindrical cell map will meet that need. For example, in Fig. 19, reducing the height to 0.5 mm instead of 5 mm results in a very large change, as can be seen in Table 14. Gears with a height of 5 mm only achieve a volume reduction of 23.6% but displacement up to 33.2% (Table 14, No. 1) compared to solid gears, while gears adopting 0.5 mm height achieve a volume reduction of 22.45% and displacement of 09.48% (Table 14, No. 11). Clearly, the lower the height of the unit cell is, the more the volume reduction and displacement reduction can increase, but it should be selected to ensure manufacturability

To test the research results for large gears, we design some new spur gear sizes with such parameters as: normal module $m = 3$ mm, normal pressure angle $\alpha = 200$, number of teeth $n = 40$, face width $b = 15$ mm, torque = 27 Nm; and the other one: normal module $m = 5$ mm, normal pressure angle $\alpha = 200$, number of teeth $n = 40$, face width $b = 25$ mm, torque = 125 Nm. After comparing the simulation results of the gear with a similar volume reduction of the gear in Table 14 No. 5, the results are as shown in Table 15 and Table 16. The results show that, even if the small gear is not capable of precision fabrication, this formula can apply to large gears. As can be seen in the table below, large gears with a pitch diameter of 120 mm (Torque=27 Nm) or 200 mm (Torque=125 Nm) still ensure displacement and stress.

The displacement increases by 18% ($d = 120$ mm) and 19% ($d=200$ mm) compared to the gear Table 14 No. 5, which is initially 15.8%, and stress and strain increase to approximately equal to that of a solid gear. Therefore, when at a larger size, the gear with the same configuration will no longer be as stiff and durable as the original. Applying the research results to adjust the control variables will obtain the desired stiffness and strength (Table 16 No. 2). Finally, the gear in Table 16 No. 1 was chosen for additive manufacture, as shown in Fig. 19 and Fig. 20.

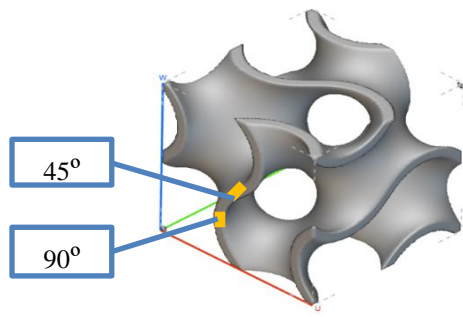


Fig. 18. Force distribution positions in Gyroid unit cell

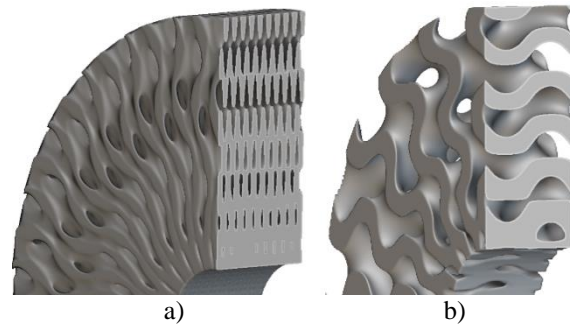


Fig. 19. Cross-section of TPMS structure with a height of 0.5 mm (a) and 5 mm (b)

Table 14. The results table simulates several configurations of input parameters to see the potential of changing the unit cell height, sorted in descending order D/D_0

No.	R	H	A	T	R_V	D	D/D_0	ε	σ
0	Full Gear				0	0.0277	1	0.00734	51.6650
1	5	5	20	1.5	0.2361	0.0369	1.3322	0.00724	42.9839
2	6	0.8	20	0.8	0.2752	0.0328	1.1855	0.00607	38.3857
3	7	0.9	30	0.8	0.2518	0.0328	1.1849	0.00833	45.2538
4	6	0.6	15	0.8	0.2748	0.0323	1.1651	0.00622	43.2415
5	8	0.9	25	0.9	0.2464	0.0321	1.1583	0.00599	34.0016
6	6	0.5	20	0.7	0.2628	0.0318	1.1465	0.00579	36.3578
7	6	0.6	25	0.7	0.2567	0.0317	1.1450	0.00544	30.8905
8	7	0.5	25	0.7	0.2503	0.0310	1.1206	0.00633	39.9433
9	8	0.9	35	0.9	0.1862	0.0307	1.1100	0.00547	35.9770
10	6	0.9	25	0.9	0.1952	0.0306	1.1060	0.01010	43.2814
11	6	0.5	25	0.7	0.2245	0.0303	1.0948	0.00599	37.5997
12	6	0.9	35	0.9	0.1321	0.0298	1.0746	0.00646	42.2791

Table 15: Large gear ($d = 120$ mm) simulation result

No.	R	H	A	T	R_V	D	D/D_0	ε	σ
0	Full Gear				0	0.0820	1	0.0073	42.2918
1	24	2.7	25	2.7	0.2486	0.0960	1.1698	0.0074	41.5751

Table 16. Large gear ($d = 200$ mm) simulation result

No.	R	H	A	T	R_v	D	D/D_0	ε	σ
0	Full Gear				0	0.1359	1	0.00795	48.0918
1	40	4.5	25	4.5	0.2486	0.1619	1.1914	0.00715	47.4175
2	20*	2.5	25	3	0.2380	0.1553	1.1430	0.00606	43.3903
* R=40 mm occurs the error (black areas appear), problem solved when reducing R=20 mm									



Fig. 20. Gear sample



Fig. 21. Close-up image

4. CONCLUSIONS

The PEEK gear, applying the TPMS Gyroid structure, is designed and simulated in the finite element model, and then based on experimental design models such as Taguchi and FCCCD to evaluate and compare the data with solid gears (VDI2736).

- The Gyroid structure is the most efficient in terms of mass optimization while preserving the mechanical properties of the gears. Six different TPMS constructs were investigated using the Taguchi method and were retested. The aim is to find a structure with guaranteed mechanical properties but with the highest volume reduction, by assessing the influence of factors on the ratio coefficients between displacement, strain, and stress on the volume reduction. The result reveals that the structural type of factor has the most significant influence, and the Gyroid structure has the lowest ratio of displacement, stress, and strain to volume reduction.

- The input parameters have a robust correlation with the volume reduction and displacement, from which the variables to be fixed can be determined, and the variables can be fine-tuned to achieve stiffness and desired volume reduction. When choosing a lower unit cell height, the stiffness of the gear increases. However, it is necessary to choose a combination with other variables to ensure the ability to build, mesh and fabricate the structure. The errors in structural modeling are not yet controllable, but simply adjusting the controlled variables will eliminate the problems.

- Volume reduction and displacement are more than 90% correlated with each other; the larger the volume reduction, the greater the displacement. To have a high-volume reduction but low displacement, it is necessary to adjust the input parameters reasonably and

scientifically based on the regression equation. This is an advantage when topology uses lattice structures because it can be easily controlled to achieve the desired volume reduction and stiffness. In contrast, the input parameters and volume reduction were not correlated with strain and stress. In most cases, lower strain and stress will be obtained than VDI2736 gear, but it will be difficult to control when there is no correlation with input parameters, only stress and strain can be guaranteed to be not greater than solid gear if the volume reduction does not exceed 30%.

- The small gear is not capable of precision fabrication, but this design method is proven for larger gears. The desired configuration in small diameters does not guarantee mechanical properties when applied to larger gears, but the design variables can still be adjusted to achieve the desired results.

ACKNOWLEDGEMENTS

We acknowledge Ho Chi Minh City University of Technology (HCMUT), VNU-HCM for supporting this study.

REFERENCES

- [1] AGMA 920-B15, *Materials for Plastic Gears*, in American Gear Manufacturers Association, 1001 N. Fairfax Street, Suite 500, Alexandria, Virginia 22314. Available: <http://www.agma.org>.
- [2] DAVIS J.R., 2005, Plastics, in *Gear Materials, Properties, and Manufacture*, J.R. Davis, Ed. ASM International, 77–88.
- [3] VDI 2736 Sheet 1, 2016, *Thermoplastic Gear Wheels – Materials*, Material Selection, Production Methods, Production Tolerances, Form Design. Beuth Verlag.
- [4] STARZHINSKY V.E., 2013, *Polymer Gears*, in *Encyclopedia of Tribology*, Q. J. Wang and Y.-W. Chung, Eds. Springer, 2592–2602. <https://doi.org/10.1007/978-0-387-92897-5>.
- [5] LI D., LIAO W., DAI N., DONG G., TANG Y., XIE Y.M., 2018, *Optimal Design and Modeling of Gyroid-Based Functionally Graded Cellular Structures for Additive Manufacturing*, *Comput. Des.*, <https://doi.org/10.1016/j.cad.2018.06.003>.
- [6] KUO Y.H., CHENG C.C., LIN Y.S., SAN C.H., 2017, *Support Structure Design in Additive Manufacturing Based on Topology Optimization*, *Struct. Multidiscip. Optim.*, 57/1, 183–195, Jul. 2017, <https://doi.org/10.1007/S00158-017-1743-Z>.
- [7] NAZIR A., ABATE K.M., KUMAR A., JENG J.Y., 2019, *A State-of-the-Art Review on Types, Design, Optimization, and Additive Manufacturing JENG of Cellular Structures*, *Int. J. Adv. Manuf. Technol.* 3489–3510, 104/9, Jul. 2019, <https://doi.org/10.1007/S00170-019-04085-3>.
- [8] WU L. *et al.*, 2018, *Optical Performance Study of Gyroid-Structured TiO₂ Photonic Crystals Replicated from Natural Templates Using a Sol-Gel Method*, *Adv. Opt. Mater.*, 6/21, <https://doi.org/10.1002/ADOM.-201800064>.
- [9] WESTER T., 2002, *Nature Teaching Structures*: *Int. J. Sp. Struct.*, 17/2–3, 135–147, <https://doi.org/10.1260/026635102320321789>.
- [10] DE PASQUALE G., MONTEMURRO M., 2018, *A Catapano, G. Bertolino, and L. Revelli, Cellular Structures from Additive Processes: Design, Homogenization and Experimental Validation*, *Procedia Struct. Integr.*, 8, 75–82, <https://doi.org/10.1016/J.PROSTR.2017.12.009>.
- [11] RIVA L., GINESTRA P.S., CERETTI E., 2021, *Mechanical Characterization and Properties of Laser-Based Powder Bed-Fused Lattice Structures: a Review*, *Int. J. Adv. Manuf. Technol.*, 113, 649–671, <https://doi.org/10.1007/S00170-021-06631-4>.
- [12] AL-KETAN O., AL-RUB R.K.A., ROWSHAN R., 2017, *Mechanical Properties of a New Type of Architected Interpenetrating Phase Composite Materials*, *Adv. Mater. Technol.*, 2/2, Feb. 2017, <https://doi.org/10.1002/ADMT.201600235>.
- [13] DU PLESSIS A., YADROITSAVA I., YADROITSEV I., LE ROUX S.G., BLAINE D.C. 2018, *Numerical Comparison of Lattice Unit Cell Designs for Medical Implants by Additive Manufacturing*, 13/4, 266–281, Oct. 2018, <https://doi.org/10.1080/17452759.2018.1491713>.

- [14] YAN C., HAO L., HUSSEIN A., RAYMONT D., 2012, *Evaluations of cellular lattice structures manufactured using selective laser melting*, Int. J. Mach. Tools Manuf., 62, 32–38, <https://doi.org/10.1016/J.IJMACHTOOLS.2012.06.002>.
- [15] BENEDETTI M., DU PLESSIS A., RITCHIE R.O., DALLAGO M., RAZAVI S.M.J., BERTO F., 2021, *Architected Cellular Materials: A Review On Their Mechanical Properties Towards Fatigue-Tolerant Design And Fabrication*, Mater. Sci. Eng. R Reports, 144, 100606, Apr. 2021, <https://doi.org/10.1016/J.MSER.2021.100606>.
- [16] TAO W., LEU M.C., 2016, *Design of Lattice Structure for Additive Manufacturing*, Int. Symp. Flex. Autom., 325–332, Dec. 2016, <https://doi.org/10.1109/ISFA.2016.7790182>.
- [17] NAGESHA B.K., DHINAKARAN., VARSHA SHREE V.M., MANOJ KUMAR K.P., CHALAWADI D., SATHISH T., 2020, *Review on characterization and impacts of the lattice structure in additive manufacturing*, Mater. Today Proc., 21, 916–919, <https://doi.org/10.1016/J.MATPR.2019.08.158>.
- [18] BARBA D., ALABORT E., R.C. REED, 2019, *Synthetic Bone: Design by Additive Manufacturing*, Acta Biomater., 97, 637–656, <https://doi.org/10.1016/J.ACTBIO.2019.07.049>.
- [19] ABUEIDDA D.W., ELHEBEARY M., (ANDREW) SHIANG C.S., PANG S., Abu Al-RUB., R.K., JASIUK I.M., 2019, *Mechanical Properties of 3D Printed Polymeric Gyroid Cellular Structures: Experimental and finite element study*, Mater. Des., 165, 107597, <https://doi.org/10.1016/J.MATDES.2019.107597>.
- [20] BIROSZ M.T., LEDENYÁK D., ANDÓ M., 2022, *Effect of FDM Infill Patterns on Mechanical Properties*, Polym. Test., 13, 107654, <https://doi.org/10.1016/J.POLYMERTESTING.2022.107654>.
- [21] BULDUK M.E., ÇALIŞKAN C.İ., COŞKUN M., ÖZER G., KOÇ E., 2021, *Comparison of the Effect of Different Topological Designs and Process Parameters on Mechanical Strength in Gears*, Int. J. Adv. Manuf. Technol. 2021 1199, 119/9, 6707–6716, <https://doi.org/10.1007/S00170-021-08405-4>.
- [22] LOC N.H., T. HUNG Q., 2021, *Optimization of Cutting Parameters on Surface Roughness and Productivity when Milling Wood Materials*, J. Mach. Eng., 21/4, 72–89, <https://doi.org/10.36897/JME/144426>.
- [23] MALÁKOVÁ S., PUŠKÁR, FRANKOVSKÝ M.P., SIVÁK S., HARACHOVÁ D., 2021, *Influence of the Shape of Gear Wheel Bodies in Marine Engines on the Gearing Deformation and Meshing Stiffness*, J. Mar. Sci. Eng., 9, 1060, 9/10, 1060, Sep. 2021, <https://doi.org/10.3390/JMSE9101060>.